Applied Physics Express **10**, 037302 (2017)
https://doi.org/10.7567/APEX.10.037302

Multimode acoustic transparency and slow sound effects in hybrid subwavelength resonators

Yu-Qiang Deng[1], Dong-Xiang Qi[1,2*], Ming-Jun Tuo[1], Lian-Zi Liu[1], Rui-Li Zhang[1], Ru-Wen Peng[1*], and Mu Wang[1]

[1]*National Laboratory of Solid State Microstructures and School of Physics, Collaborative Innovation Center of Advanced Microstructures, Nanjing University, Nanjing 210093, China*
[2]*School of Science, Jiangnan University, Wuxi 214122, China*

*E-mail: dongxiang87@gmail.com; rwpeng@nju.edu.cn

Received November 11, 2016; accepted January 27, 2017; published online February 13, 2017

In this paper, we demonstrate that a series of hybrid Helmholtz resonators, which introduce "acoustic transparent atoms", "acoustic nontransparent atoms", and "acoustic quasitransparent atoms" simultaneously, can generate multimode acoustic transparency and the slow sound effect. Dual-mode acoustic transparency can be achieved by employing a waveguide incorporating three different Helmholtz resonators. Additional modes are introduced by adding further acoustic quasitransparent atoms. This can be explained by the destructive interference among different resonators. Furthermore, slow sound propagation is demonstrated in our multimode acoustic transparency systems by employing time-domain simulations. Our results may have potential applications for sound control in one-dimensional waveguides.

In recent years, we have seen an increasing interest in the phenomenon of slow sound[1–9] in analogy with its photonic counterparts. Strong dispersion is required to decrease the group velocity of acoustic waves, which could be produced by detuned Helmholtz resonators,[7,9] a sonic crystal waveguide,[3] lined ducts,[4] and so forth. Very recently, slow surface acoustic waves have been achieved in periodically corrugated metawires for highly localized modes.[2] These studies have different focuses and applications. A linear waveguide, obtained by removing a row in a sonic crystal, can introduce a narrow defect mode within the bandgaps and the slow sound effect.[3] This can be used for gas sensing as the group velocity of sound waves is sensitive to the gas density.[3] Recently, the dissipation of slow sound propagation has been studied to design a subwavelength acoustic absorber.[5,6] By decreasing the effective sound velocity, the device thickness could be markedly reduced, thereby paving the way for low-frequency sound attenuation and mufflers.[5,6] In particular, detuned acoustic resonators could be utilized as narrow-band filters and switches to induce the phenomenon of acoustic transparency and slow sound propagation,[7,9] which is analogous to the effect of electromagnetically induced transparency (EIT).

EIT is a quantum interference phenomenon in three-level atomic systems,[10] in which the transmission of light is enhanced and the group velocity is decreased. Recently, with the development of plasmonics and metamaterials, researchers have realized EIT-like phenomena in classical systems at different bands.[11–17] However, as acoustic wave, they have started to obtain analogies between EIT-like phenomena and acoustic systems. The development of acoustic metamaterials,[18–23] which has greatly expanded the functionality of traditional acoustic materials, has led to the realization that it is possible to introduce EIT-like phenomena in acoustics by different methods. For example, Liu et al. observed an acoustic EIT-like phenomenon in differently oriented arrays of square rods,[8] which could be explained by the coupling of resonant modes with different Q factors. Santillán and Bozhevolnyi utilized detuned Helmholtz resonators (HRs) to achieve an EIT-like phenomenon,[9] which is due to Fano-like interference between two different resonators. Very recently, in order to expand the applications of the EIT-like phenomenon in metadevices, this phenomenon has been extended to dual modes or multiple modes in optics.[24–27] However, in acoustics, only a single mode of EIT-like behavior has been demonstrated, thereby possibly limiting its practical applications.

This prompted us to attempt to achieve the dual-mode and multimode EIT-like phenomenon in a one-dimensional (1D) acoustic waveguide with hybrid HRs and we describe our preliminary results in this Letter. It is known that EIT-like behavior can be generated from the destructive interference of two resonators. In optics, these two resonators are known as "bright atoms" and "dark atoms".[12–15,24] Analogy to the optical system in Ref. 24, we introduce "transparent atoms", "nontransparent atoms", and "quasitransparent atoms" in acoustics to realize dual-mode and multimode EIT-like phenomena, demonstrated by both a simple analytical model and finite element simulations. These phenomena can be interpreted as the coupling of different resonators. Furthermore, by using time-domain simulations, we demonstrate that slow sound propagation can exist in the multimode EIT-like phenomenon. Our results may overcome the limits of single-mode EIT-like behavior for applications in miniaturized acoustic devices, noise attenuation, multiple band filters, and so forth.

Here, we first study the transmission properties of acoustic waveguides to which three different single HRs are attached, as illustrated in Figs. 1(a)–1(c). The diameter of the waveguide is 2 cm and the three HRs have the same parameters for the necks and the same radius of the resonators, whereas their heights are different. These different resonators are denoted as A_1, A_2, and A_3, to indicate that they introduce three different resonant frequencies as shown in Figs. 1(a)–1(c). Then, the three HRs are attached to the 1D waveguide, separated by 120° in the cross-sectional plane, around the same position as shown in Fig. 1(d). In the following, we first study the transmission properties of this structure using an analytic model. As the size of the resonator is much smaller than the wavelength, each resonator can be treated as an impedance element, and the impedance is[9]

$$Z_i = R_i + j\left(\omega M_i - \frac{1}{\omega C_i}\right), \tag{1}$$

where ω represents the angular frequency, and R_i, M_i, and C_i signify the acoustic resistance, inertance, and stiffness, respectively. Here, $M_i = \rho_0 l/S$, where $l = l_0 + \Delta l$ and S are

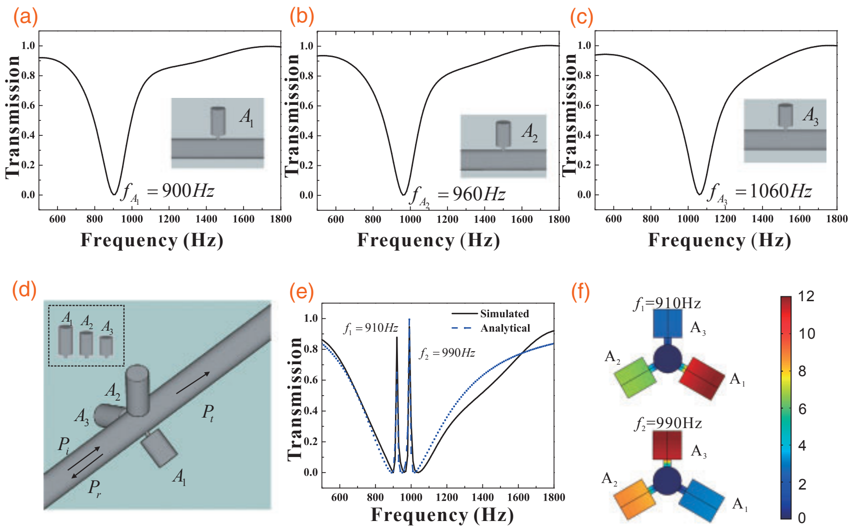

Fig. 1. Transmission properties: (a)–(c) three different Helmholtz resonators with resonant frequencies of 900, 960, and 1060 Hz, respectively. The inset figures show the schematic diagrams of these three resonators attached to a waveguide. (d) System combined with three HRs for realizing dual-mode EIT-like phenomenon. (e) Transmission curves of the system in (d) obtained from both analytical calculations (blue dashed lines) and finite element simulations (black solid lines). There are two transparent peaks at 910 and 990 Hz. (f) Simulated intensity distributions at the frequencies of the two transparent peaks in (e).

the effective length and the area of the bottom of the neck. In addition, $C_i = V_i/\rho_0 c_0^2$, where V_i represents the volume of the resonator. From Eq. (1), we can see that, owing to the difference in the heights of the resonators, the resonant frequencies of these HRs are different. In this system, the incident, reflected, and transmitted waves can be expressed as

$$\begin{cases} p_{\rm i} = p_{\rm i0} e^{j(\omega t - kx)} \\ p_{\rm r} = p_{\rm r0} e^{j(\omega t + kx)} \\ p_{\rm t} = p_{\rm t0} e^{j(\omega t - kx)} \end{cases}. \tag{2}$$

Here, $p_{\rm i0}$, $p_{\rm r0}$, and $p_{\rm t0}$ represent the amplitudes of the incident, reflected, and transmitted waves, respectively, and k is the wave vector of the incident wave. Furthermore, the acoustic wave at the entry of each HR can be expressed as

$$p_{A_i} = p_{A_i 0} e^{j(\omega t - kr)}. \tag{3}$$

Here, $i = 1$, 2, and 3 represent the three different HRs. Then, we apply Eqs. (2) and (3) to the continuous boundary conditions of pressure and volume velocity as

$$\begin{aligned} p_{\rm i} + p_{\rm r} = p_{\rm t} = p_{A_i} \\ U_i + U_r = \sum_i U_{A_i} + U_t. \end{aligned} \tag{4}$$

Finally, the transmission coefficient can be derived as

$$T = \frac{2Z_A}{Z + 2Z_A}, \tag{5}$$

in which $Z = \rho_0 c_0/S$ is the impedance of air and S is the cross-sectional area of the waveguide. $Z_A = Z_1 Z_2 Z_3/(Z_1 Z_2 + Z_2 Z_3 + Z_1 Z_3)$ is the shunt impedance of these three HRs.

Equation (5) enables us to calculate the transmission spectra, represented by the blue dashed lines in Fig. 1(e), in which two EIT-like transparent peaks can be seen at 910 and 990 Hz. Then, this dual-mode EIT-like phenomenon is confirmed by calculating the transmission curve through finite element simulation (COMSOL Multiphysics 3.5a), shown in Fig. 1(e) as black solid lines. It is clear that the analytical prediction corresponds well to the simulation results. To further understand the origin of this acoustic dual-mode EIT-like behavior, the intensity distribution of the cross section is calculated at the two transparent peaks as shown in Fig. 1(f). At 910 Hz, the energy is mainly localized in A_1 and A_2; the EIT-like transmission peak is due to the cancelation of opposite contributions from A_1 and A_2, with opposite signs of detuning from the probe frequency; whereas at 990 Hz, the transmission peak is due to the opposite contributions from A_2 and A_3. Analogous to optics, we can consider A_1, A_2, and A_3 as non-transparent atoms, quasitransparent atoms, and transparent atoms in acoustics, respectively. The Fano-like interference between the two different resonators gives rise to the dual-mode EIT-like phenomenon. The resonators have similar Q-factors, which results in the weak asymmetry of the transmission line. Furthermore, if we increase the losses of the resonators, the Q-factors will slightly decrease, resulting in less sharpness of the EIT-like peaks. We therefore propose a new approach based on the premise that the multimode EIT-like behavior can be realized by introducing additional quasitransparent atoms.

According to the same principle, we can increase the number of quasitransparent atoms, which are the different Helmholtz resonators in our system, to achieve three-mode, four-mode, and five-mode EIT-like behaviors, as shown in Fig. 2. The black solid curves represent the simulated transmission results, and the figures appearing as insets show the corresponding structures. We can see that multiple modes can be realized by adding a number of quasitransparent atoms. In addition, the energy distributions at different transparent peaks are shown in Fig. 3 for improved understanding. The difference in the field distributions at different frequencies enabled us to confirm that an increase in the number of HRs with different resonant frequencies can achieve multimode EIT-like behavior, in which the destructive coupling between different adjacent HRs plays a key role.

In another respect, we also demonstrate slow sound effects in the dual-mode and multimode systems. The results are enhanced by arranging four cells of the hybrid HRs like that shown in Fig. 1(d). These cells are separated by 5 cm along

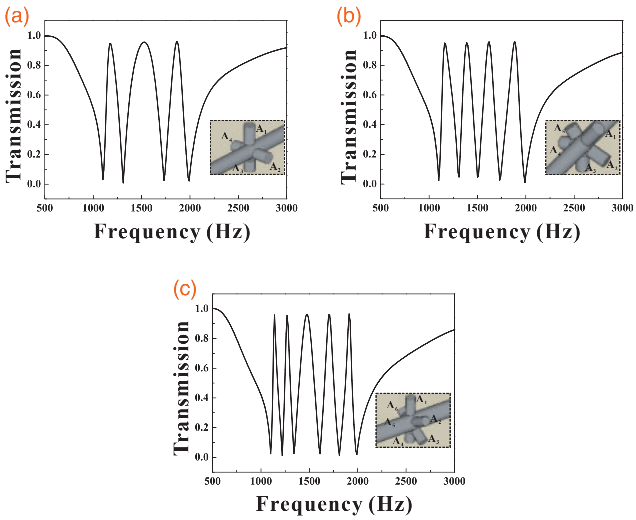

Fig. 2. Transmission spectra of (a) three-, (b) four-, and (c) five-mode EIT-like phenomena. The inset figures are the schematic diagrams of each phenomenon.

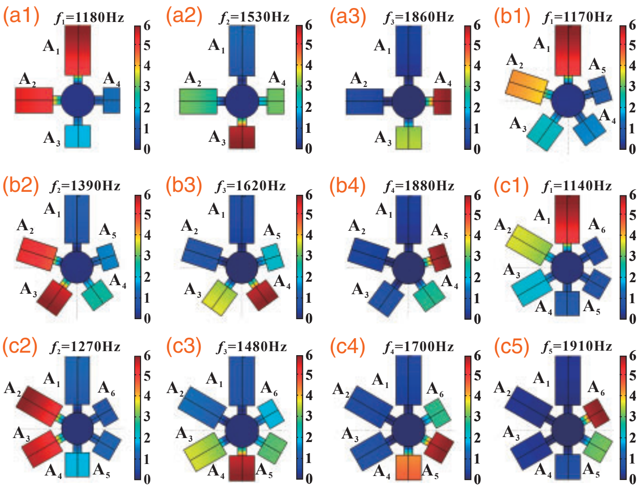

Fig. 3. Simulated intensity distributions of different resonant modes for (a1)–(a3) three-mode, (b1)–(b4) four-mode, and (c1)–(c5) five-mode EIT-like phenomena.

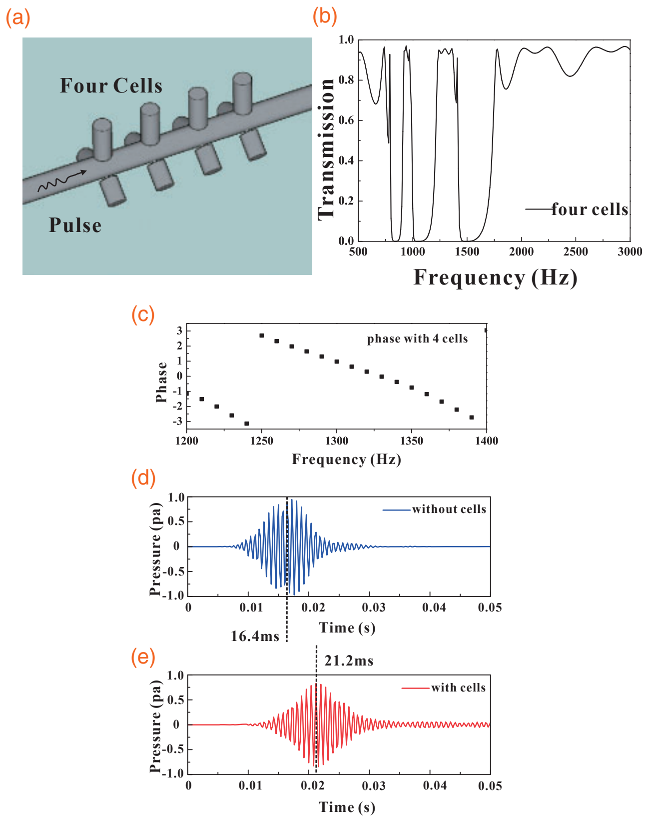

Fig. 4. (a) Schematic diagram for the demonstration of slow sound propagation in the dual-mode EIT-like systems, in which four cells of dual-mode EIT-like structures are arranged along the acoustic waveguide, separated by 5 cm. (b, c) Transmission and phase curves for the system in (a), respectively. (d, e) Simulated signal of transmitted waves without and with cells, respectively. In comparison, there is a 4.8 ms delay.

the waveguide as shown in Fig. 4(a). The transmission property of this structure can be seen in Fig. 4(b), obtained through finite element simulations. Here, we can also obtain two transparent peaks centered at 940 and 1300 Hz, as discussed above. In addition, the phase spectra are also calculated as shown in Fig. 4(c). The strong dispersion of the phase spectra indicates that the sound velocity can be largely decreased through this structure.

We know that when sound waves pass through the one-dimensional waveguide system, the HR series can be regarded as a one-dimensional acoustic metamaterial. Furthermore, the effective refractive index has the following relationship with the phase of the transmitted wave:[28)]

$$n(\omega) = -\frac{\Phi(\omega)}{\omega(N-1)l_c/c}. \qquad (6)$$

Here, n and Φ represent the effective refractive index and the phase of the transmitted wave, respectively. $N = 4$ is the number of cells, $l_c = 5$ cm is the distance between adjacent cells, and $c = 343$ m/s is the velocity of sound in air. Equation (6) enables us to calculate the effective group refractive index via $n_g(\omega) = n(\omega) + \omega dn(\omega)/d\omega$. Thus, as we can see from Fig. 4(c), the phase of the transmitted wave varies quite severely, and this enables us to obtain the phase slope and predict that the group refractive index n_g can reach 12.6 at the second transparent peak (1300 Hz). Accordingly, the group velocity of sound can be largely decreased. Here, we predict that the group velocity of sound can be decreased as $c_g = c/n_g$.

Our above prediction was confirmed by carrying out a time-domain simulation using COMSOL Multiphysics 3.5a. Here, we set the incidence as a Gaussian pulse centered at the frequency of the second transparent peak (1300 Hz), as shown in Fig. 4(b). Then, the acoustic signal is received at a distance of 30 cm behind the structures. The simulation results are shown in Figs. 4(d) and 4(e). In contrast, Fig. 4(d) shows the signal of a sound pulse that passed through a pipe without cells and Fig. 4(e) is the result after passing through four cells. This indicates that, without cells, the maximum of the envelope of the signal is reached at $t = 16.4$ ms, whereas with cells, the maximum value of the envelope is reached at $t = 21.2$ ms. Thus, a wave packet will experience a delay of 4.8 ms when traversing cells with a length of $(N-1)l_c = 15$ cm. Then, we can calculate the group velocity at 1300 Hz through the four cells as $c_g = 28.6$ m/s, thereby obtaining a group refractive index of $n_g = 12$, which agrees well with the above prediction from the phase spectra. We also confirmed the slow sound effect at the frequency of the first transparent peak (940 Hz), where the group refractive index equals 25.

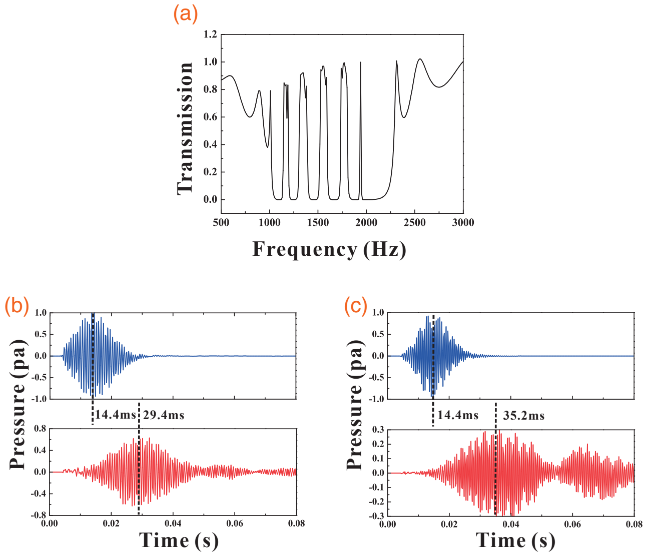

Fig. 5. (a) Transmission spectra of the five-mode EIT-like phenomenon with four cells. Slow sound effects at frequencies of (b) 1340 and (c) 1550 Hz. The blue and red traces are the results without and with cells, with time delays of 15 and 20.8 ms, respectively.

Here, we have demonstrated the slow sound effect in the structure producing our dual-mode EIT-like phenomenon.

Furthermore, by the same method, we demonstrate that the structure exhibiting the multimode EIT-like behavior can also decrease the acoustic signal velocity. Here, in the case of five modes, four cells are arranged with a 5 cm separation — the transmission curve can be seen in Fig. 5(a). The transmitted signals are simulated at the frequencies of the second and third transparent peaks. As shown in Fig. 5(b), at a frequency of 1340 Hz, the situation with four cells results in a 15 ms delay compared with the situation without cells. Moreover, in Fig. 5(c), at a frequency of 1550 Hz, there is a 20.8 ms delay accordingly. Therefore, the corresponding group refractive index reaches approximately 35 and 65. Here, we have demonstrated that a multimode slow sound effect will also exist in our hybrid subwavelength resonators.

In summary, we have demonstrated that multimode acoustic transparency and the slow sound effect can be realized in a one-dimensional waveguide to which hybrid Helmholtz resonators are attached. Through analytical calculation, we show that the dual-mode EIT-like phenomenon can be achieved with the waveguide attached to three different HRs. In addition, the results are verified by conducting a finite element simulation. The simulated intensity distribution indicates that the dual-mode behavior results from the destructive interference between two different adjacent resonators. In analogy to the EIT-like phenomenon in optics, we refer to the different HRs as transparent atoms, nontransparent atoms, and quasi-transparent atoms in acoustics. Furthermore, the multimode EIT-like behavior can be achieved by introducing additional acoustic quasitransparent atoms in our structure. On the other hand, slow sound propagations are demonstrated in our structures. In the case of dual-mode transmission, the time-domain simulation demonstrates that the group velocity of the Gaussian pulse is decreased by an order of magnitude. In addition, we also demonstrate the existence of a multimode slow sound effect in the case of the multimode EIT-like phenomenon. Our results may be used for sound control in acoustic waveguides, thus providing a potential application for integrated and miniaturized acoustic devices.

Acknowledgments This work was supported by the National Natural Science Foundation of China (Grant Nos. 11634005, 61475070, 11504136, 11474157, 11674155, and 11621091), and the Natural Science Foundation of Jiangsu Province of China (Grant No. BK20140127).

1) W. M. Robertson, C. Baker, and C. Brad Bennett, Am. J. Phys. **72**, 255 (2004).
2) J. Christensen, P. A. Huidobro, L. Martín-Moreno, and F. J. García-Vidal, Appl. Phys. Lett. **93**, 083502 (2008).
3) A. Cicek, O. A. Kaya, M. Yilmaz, and B. Ulug, J. Appl. Phys. **111**, 013522 (2012).
4) Y. Aurégan and V. Pagneux, J. Acoust. Soc. Am. **138**, 605 (2015).
5) J.-P. Groby, R. Pommier, and Y. Aurégan, J. Acoust. Soc. Am. **139**, 1660 (2016).
6) Y. Aurégan, M. Farooqui, and J.-P. Groby, J. Acoust. Soc. Am. **139**, EL149 (2016).
7) X. Li, C. Xue, L. Fan, S. Zhang, Z. Chen, J. Ding, and H. Zhang, Appl. Phys. Lett. **108**, 231904 (2016).
8) F. M. Liu, M. Z. Ke, A. Q. Zhang, W. J. Wen, J. Shi, Z. Y. Liu, and P. Sheng, Phys. Rev. E **82**, 026601 (2010).
9) A. Santillán and S. I. Bozhevolnyi, Phys. Rev. B **84**, 064304 (2011).
10) S. E. Harris, J. E. Field, and A. Imamoglu, Phys. Rev. Lett. **64**, 1107 (1990).
11) N. Papasimakis, V. A. Fedotov, N. I. Zheludev, and S. L. Prosvirnin, Phys. Rev. Lett. **101**, 253903 (2008).
12) Y. Sun, H. Jiang, Y. Yang, Y. Zhang, H. Chen, and S. Zhu, Phys. Rev. B **83**, 195140 (2011).
13) S. Y. Chiam, R. Singh, C. Rockstuhl, F. Lederer, W. Zhang, and A. A. Bettiol, Phys. Rev. B **80**, 153103 (2009).
14) L. Qin, K. Zhang, R. W. Peng, X. Xiong, W. Zhang, X. R. Huang, and M. Wang, Phys. Rev. B **87**, 125136 (2013).
15) P. Tassin, L. Zhang, T. Koschny, E. N. Economou, and C. M. Soukoulis, Phys. Rev. Lett. **102**, 053901 (2009).
16) S. Zhang, D. A. Genov, Y. Wang, M. Liu, and X. Zhang, Phys. Rev. Lett. **101**, 047401 (2008).
17) N. Liu, L. Langguth, T. Weiss, J. Kastel, M. Fleischhauer, T. Pfau, and H. Giessen, Nat. Mater. **8**, 758 (2009).
18) N. Fang, D. Xi, J. Xu, M. Ambati, W. Srituravanich, C. Sun, and X. Zhang, Nat. Mater. **5**, 452 (2006).
19) Z. Yang, J. Mei, M. Yang, N. Chan, and P. Sheng, Phys. Rev. Lett. **101**, 204301 (2008).
20) J. Li, L. Fok, X. Yin, G. Bartal, and X. Zhang, Nat. Mater. **8**, 931 (2009).
21) J. Zhu, J. Christensen, J. Jung, L. Martin-Moreno, X. Yin, L. Fok, X. Zhang, and F. J. Garcia-Vidal, Nat. Phys. **7**, 52 (2011).
22) S. A. Cummer, B. I. Popa, D. Schurig, D. R. Smith, J. Pendry, M. Rahm, and A. Starr, Phys. Rev. Lett. **100**, 024301 (2008).
23) X. Zhu, B. Liang, W. Kan, X. Zou, and J. Cheng, Phys. Rev. Lett. **106**, 014301 (2011).
24) K. Zhang, C. Wang, L. Qin, R. W. Peng, D. H. Xu, X. Xiong, and M. Wang, Opt. Lett. **39**, 3539 (2014).
25) J. Kim, R. Soref, and W. R. Buchwald, Opt. Express **18**, 17997 (2010).
26) L. Zhu, F. Y. Meng, J. H. Fu, Q. Wu, and J. Hua, Opt. Express **20**, 4494 (2012).
27) J. Chen, C. Wang, R. Zhang, and J. Xiao, Opt. Lett. **37**, 5133 (2012).
28) A. Santillán and S. I. Bozhevolnyi, Phys. Rev. B **89**, 184301 (2014).